AD-A127 604 EVALUATING THE DETECTABILITY OF GAUSSIAN STOCHASTIC SIGNALS BY STEEPEST-D.. (U) CALIFORNIA UNIV SAN DIEGO LA JOLLA DEPT OF ELECTRICAL ENGINEE.. C W HELSTROM 1983 1/1

UNCLASSIFIED AFOSR-TR-83-0285 AFOSR-82-0343 F/G 12/1 NL

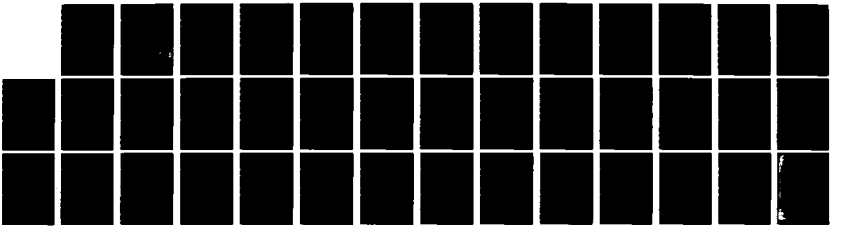

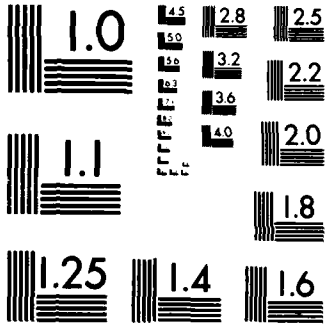

UNCLASSIFIED

SECURITY CLASSIFICATION OF THIS PAGE (When Data Entered)

REPORT DOCUMENTATION PAGE		READ INSTRUCTIONS BEFORE COMPLETING FORM
1. REPORT NUMBER AFOSR-TR- 83-0285	2. GOVT ACCESSION NO. A127604	3. RECIPIENT'S CATALOG NUMBER
4. TITLE (and Subtitle) EVALUATING THE DETECTABILITY OF GAUSSIAN STOCHASTIC SIGNALS BY STEEPEST-DESCENT INTEGRATION		5. TYPE OF REPORT & PERIOD COVERED TECHNICAL
		6. PERFORMING ORG. REPORT NUMBER
7. AUTHOR(s) Carl W. Helstrom		8. CONTRACT OR GRANT NUMBER(s) AFOSR-82-0343
9. PERFORMING ORGANIZATION NAME AND ADDRESS Department of Electrical Engineering & Computer Sciences, University of California, San Diego, La Jolla, CA 92093		10. PROGRAM ELEMENT, PROJECT, TASK AREA & WORK UNIT NUMBERS PE61102F; 2304/A5
11. CONTROLLING OFFICE NAME AND ADDRESS Mathematical & Information Sciences Directorate Air Force Office of Scientific Research Bolling AFB DC 20332		12. REPORT DATE 1983
		13. NUMBER OF PAGES 37
14. MONITORING AGENCY NAME & ADDRESS (if different from Controlling Office)		15. SECURITY CLASS. (of this report) UNCLASSIFIED
		15a. DECLASSIFICATION DOWNGRADING SCHEDULE

16. DISTRIBUTION STATEMENT (of this Report)

Approved for public release; distribution unlimited.

17. DISTRIBUTION STATEMENT (of the abstract entered in Block 20, if different from Report)

18. SUPPLEMENTARY NOTES

To appear in IEEE Trans. Aerosp. & Electr. Sys.

19. KEY WORDS (Continue on reverse side if necessary and identify by block number)

20. ABSTRACT (Continue on reverse side if necessary and identify by block number)

It is shown how to compute the detection probability of certain signals by numerical integration of the Laplace inversion integral involving the characteristic function or the moment-generating function of the detection statistic. The contour of integration is taken as the path of steepest descent of the integrand and is determined numerically as the integration proceeds. The method is applied to calculating the performance of the optimum detector of a Gaussian stochastic signal in white noise when the signals actually present have a different average s.n.r. from that assumed in the design. (CONTINUED)

DD FORM 1 JAN 73 1473

UNCLASSIFIED

SECURITY CLASSIFICATION OF THIS PAGE (When Data Entered)

ITEM #20, CONTINUED: Results are presented for narrowband signals with Lorentz and rectangular spectral densities. The detectability of the former is shown to be more sensitive than that of the latter to the value of the design s.n.r. The relative disadvantage of the threshold detector, also assessed by this method, is smaller for signals with a rectangular than for those with a Lorentz spectral density.

To appear in IEEE Trans. Aerosp. & Electr. S

Grant
AFOSR-82-0343

AFOSR-TR- 83-0285

Evaluating the Detectability of Gaussian Stochastic Signals by Steepest-Descent Integration

Carl W. Helstrom

Department of Electrical Engineering & Computer Sciences

University of California, San Diego

La Jolla, California 92093

Abstract

It is shown how to compute the detection probability of certain signals by numerical integration of the Laplace inversion integral involving the characteristic function or the moment-generating function of the detection statistic. The contour of integration is taken as the path of steepest descent of the integrand and is determined numerically as the integration proceeds. The method is applied to calculating the performance of the optimum detector of a Gaussian stochastic signal in white noise when the signals actually present have a different average s.n.r. from that assumed in the design. Results are presented for narrowband signals with Lorentz and rectangular spectral densities. The detectability of the former is shown to be more sensitive than that of the latter to the value of the design s.n.r. The relative disadvantage of the threshold detector, also assessed by this method, is smaller for signals with a rectangular than for those with a Lorentz spectral density.

I. Introduction

In calculating the probability of detecting a certain kind of signal by means of a certain receiver, it sometimes happens that although the characteristic function of the detection statistic is known in rather simple form, inverting it to determine the probability density function of the statistic and integrating that to find the detection probability may be quite difficult. One example is the detection of a fading radar signal by a receiver that sums, or "integrates", the quadratically rectified outputs of a matched filter following transmission of a number of radar pulses. When the fading is described as in Swerling's Cases III and IV, for instance, the average detection probability can be written down in closed form, but it is very complicated, although the characteristic function from which it is derived is relatively simple [1]. Straightforward computation with that closed form is a lengthy process when the number of pulses integrated is large, and it may require double precision in order to avoid overflow or underflow of the numbers involved.

Another example is the detection of a narrowband stochastic signal, as in radar astronomy and scatter-multipath communications [2]. When the signal can be modeled as a segment of a Gaussian stochastic process and is received in white noise, the characteristic function of the optimum detection statistic can be expressed as an infinite product involving the eigenvalues of the autocovariance function of the signal process, and the probability of detection comes out as an infinite series when this characteristic function is inverted by means of the residue theorem [3,4,5]. Computations with this series are feasible only when the number of significant eigenvalues is small, unless both the eigenvalues and the terms of the series are carried to double precision.

Problems such as these generally involve a detection statistic that can at least roughly be represented as the sum of a certain number of independent

random variables; this number can be termed the number of "degrees of freedom" in the statistic. In radar detection it is the number of pulses integrated; in detecting a stochastic signal it is the product of the bandwidth of the signal and the observation time. The inversion of the characteristic function by the residue theorem in order to determine the probability density function of the statistic, and its integration to obtain the probability of detection, become computationally the more difficult, the larger the number of degrees of freedom in the detection statistic.

The probability of detection can also be expressed as a contour integral involving the characteristic function or the moment-generating function (m.g.f.) of the detection statistic. Here we shall describe how the detection probability can be conveniently calculated by numerical evaluation of this integral along an appropriate path. The path goes through the same saddlepoint of the integrand that was featured in an approximate method for evaluating such integrals, described in [6]. By choosing the contour of integration as that along which the integrand decreases to zero most rapidly on each side of the saddlepoint, the integral can be expeditiously and accurately evaluated by applying the trapezoidal rule [7]. This contour of integration is known as the path of steepest descent.

An advantage of the method is that it can be applied when the number of degrees of freedom is arbitrarily large. The principles underlying it are lucidly explained in the book by Carrier et al. [8]. It was used in a fluid-mechanical problem by Esch [9], and a particular method for locating the path of steepest descent and numerically integrating along it was described by Rice [7]. A somewhat different method for determining the path will be presented in Section III. Because the use of steepest-descent integration to calculate detection probabilities seems not to be widely known among radar engineers and

system analysts, it will be reviewed here in terms of a particular example, that of calculating the detectability of Gaussian stochastic signals in white noise.

The optimum detector of Gaussian stochastic signals requires for its design either knowledge of or an assumption about the average signal-to-noise ratio of the signals to be detected. The performance of this optimum detector was extensively analyzed by Van Trees [5] by means of an approximation to the error probability akin to the Chernoff bound, but he assumed that the average s.n.r. of the signals actually arriving was equal to that for which the detector was designed. The performance of this detector when the average input s.n.r. differs from that assumed in the design seems not to have been studied. Here we shall show how that can be done by utilizing a new factorization of the m.g.f., which is presented in Section II, and which permits efficient calculation of the detection probability by the residue series for low values of the time-bandwidth product. Section III shows how to calculate the detection probability for arbitrarily large values of that product by steepest-descent integration. Section IV describes how to calculate the decision level required for attaining a pre-assigned false-alarm probability. The results are presented in Section V as graphs of the average input s.n.r. needed in order to attain a given pair of false-alarm and detection probabilities, as a function of the average s.n.r. for which the detector has been designed to be optimum. The results enable us in particular to assess the loss in signal detectability entailed by adopting the threshold detector, which is optimum in the limit of vanishing input s.n.r. and is simpler to construct than the detector that is optimum for finite input s.n.r. The calculations were carried out for signals with two types of spectral density, the Lorentz, which decreases to zero like $|\omega|^{-2}$ at large frequency deviation $|\omega|$ from the carrier frequency, and the rectangular,

which is confined to a finite spectral band, within which it is uniform. These two types of spectral density represent opposite extremes, bracketing spectral densities with a variety of asymptotic dependence on $|\omega|$. It is found that the detectability of signals with the Lorentz spectral density is much more sensitive to the choice of the design s.n.r. than is the detectability of signals with a rectangular spectral density.

II. The Detectability of Gaussian Stochastic Signals.

(a) The Optimum Detector

A narrowband Gaussian stochastic signal

$$s(t) = \mathrm{Re}\ [S(t)e^{i\Omega t}]$$

of carrier frequency Ω is to be detected in the presence of white Gaussian noise of unilateral spectral density N by observation of the input

$$v(t) = \mathrm{Re}\ [V(t)e^{i\Omega t}]$$

to a receiver during an interval (0,T). The complex autocovariance function of the signal is

$$\phi(t_1,t_2) = \tfrac{1}{2}E[S(t_1)S^*(t_2)], \tag{1}$$

E standing for expected value, and

$$E[S(t_1)S(t_2)] = 0.$$

The derivation of the optimum and threshold detectors is well enough known that a summary to establish notation will suffice [3,4,5].

Define hypothesis H_γ as the proposition that the complex envelope of the input v(t) to the receiver is

$$V(t) = \gamma^{\frac{1}{2}}S(t) + N(t), \tag{2}$$

where N(t) is the complex envelope of the white noise, with

$$\tfrac{1}{2}E[N(t_1)N^*(t_2)] = N\delta(t_1 - t_2),$$

$$E[N(t_1)N(t_2)] = 0. \tag{3}$$

The parameter γ measures the strength of the incoming signals relative to that of the signals for which the receiver is designed to be optimum.

The complex envelope V(t) of the input is sampled by means of a set of functions $f_k(t)$ orthonormal over the observation interval (0,T),

$$V(t) = \sum_{k=1}^{\infty} z_k f_k(t), \qquad z_k = \int_0^T f_k^*(t) V(t) dt. \tag{4}$$

By taking the $f_k(t)$ as the eigenfunctions of the kernel $N^{-1}\phi(t_1,t_2)$,

$$\lambda_k f_k(t) = N^{-1} \int_0^T \phi(t,s) f_k(s) ds, \qquad \forall k, \tag{5}$$

the complex samples $z_k = x_k + iy_k$ are statistically independent, circular-complex Gaussian random variables whose real and imaginary parts have variances

$$\tfrac{1}{2} E(z_k z_k^* | H_\gamma) = N(1+\gamma\lambda_k) \tag{6}$$

under hypothesis H_γ; the joint p.d.f. of a finite number n of them can be written

$$p_\gamma(x_1, \ldots, x_n, y_1, \ldots, y_n) = \tilde{p}_\gamma(z_1, \ldots, z_n)$$

$$= \prod_{k=1}^{n} [2\pi N(1+\gamma\lambda_k)]^{-1} \exp\left[- \frac{|z_k|^2}{2N(1+\gamma\lambda_k)} \right] \tag{7}$$

The optimum detection statistic U is proportional to the logarithm of the likelihood ratio $\tilde{p}_1/\tilde{p}_0$ in the limit $n \to \infty$,

$$U = \tfrac{1}{2} \sum_{k=1}^{\infty} \left[\frac{|z_k|^2}{N} - \frac{|z_k|^2}{N(1+\lambda_k)} \right]$$

$$= \frac{1}{2N} \sum_{k=1}^{\infty} \frac{\lambda_k |z_k|^2}{1+\lambda_k} \tag{8}$$

This statistic is compared with a decision level U_0; when $U > U_0$, the receiver decides that a signal is present. The value of U_0 is set so that the false-alarm probability $\Pr(U > U_0 | H_0)$ takes on a pre-assigned value Q_0.

We shall calculate the probability

$$Q_d(\gamma) = \Pr(U > U_0 | H_\gamma) \tag{9}$$

that the receiver decides a signal present when the one actually on hand is a realization of a narrowband Gaussian stochastic process with complex autocovariance $\gamma\phi(t_1,t_2)$. The moment-generating function (m.g.f.) of the statistic U under hypothesis H_γ is

$$h_\gamma(s) = E(e^{-sU}|H_\gamma)$$

$$= \prod_{k=1}^{\infty} [2\pi N(1+\gamma\lambda_n)]^{-1} \int_{-\infty}^{\infty}\int_{-\infty}^{\infty} \exp\left[-\frac{|z_k|^2}{2N(1+\gamma\lambda_k)} - \frac{s\lambda_k|z_k|^2}{2N(1+\lambda_k)}\right] dx_k dy_k$$

$$= \prod_{k=1}^{\infty} [1+\mu_k(\gamma)s]^{-1}, \tag{10}$$

where

$$\mu_k(\gamma) = \frac{\lambda_k(1+\gamma\lambda_k)}{1+\lambda_k}. \tag{11}$$

Then the detection probability is

$$Q_d(\gamma) = -\int_{c-i\infty}^{c+i\infty} s^{-1} h_\gamma(s) \exp(U_0 s)\, ds/2\pi j,$$

$$-\mu_1^{-1} < c < 0, \tag{12}$$

by the inversion theorem for Laplace transforms; the contour of integration runs parallel to and to the left of the imaginary axis in the complex s-plane, but to the right of the singularities of the m.g.f. $h_\gamma(s)$. By evaluating the contour integral by the residue theorem, we find

$$Q_d(\gamma) = \sum_{k=1}^{\infty} \rho_k \exp[-U_0/\mu_k(\gamma)],$$

$$\rho_k = \prod_{\substack{\ell \\ \ell \neq k}}^{\infty} \left(1 - \frac{\mu_\ell}{\mu_k}\right)^{-1} \tag{13}$$

A form often more convenient for computation arises by factoring the terms of $h_\gamma(s)$ as

$$1+\mu_k s = \frac{1+(1+s)\lambda_k+\gamma s\lambda_k^2}{1+\lambda_k} = \frac{(1+\alpha_s\lambda_k)(1+\beta_s\lambda_k)}{1+\lambda_k}, \tag{14}$$

where

$$\alpha_s = \alpha(s;\gamma) = \tfrac{1}{2}\{1+s+[(1+s)^2-4\gamma s]^{\frac{1}{2}}\},$$

$$\beta_s = \beta(s;\gamma) = \tfrac{1}{2}\{1+s-[(1+s)^2-4\gamma s]^{\frac{1}{2}}\}; \tag{15}$$

and the m.g.f. is

$$h_\gamma(s) = \frac{D(1)}{D(\alpha_s)D(\beta_s)} \tag{16}$$

in terms of the Fredholm determinant

$$D(s) = \sum_{k=1}^{\infty} (1+\lambda_k s), \tag{17}$$

associated with the integral equation (5).

At the pole $s_k = -[\mu_k(\gamma)]^{-1}$ of $h_\gamma(s)$,

$$\alpha_s = \alpha(s_k,\gamma) = \alpha_k = \frac{\gamma(1+\lambda_k)}{1+\gamma\lambda_k}, \tag{18}$$

$$\beta_s = \beta(s_k,\gamma) = -1/\lambda_k. \tag{19}$$

Thus the poles of $h_\gamma(s)$ reside in the factor $[D(\beta_s)]^{-1}$ of (16), and the residue at $s = s_k$ equals

$$\frac{D(1)}{D(\alpha_k)D'(-\lambda_k^{-1})(d\beta_s/ds)_{s=s_k}} = \frac{(1+2\gamma\lambda_k+\gamma\lambda_k^2)D(1)}{(1+\gamma\lambda_k)^2 D(\alpha_k)D'(-\lambda_k^{-1})},$$

the prime indicating the derivative $dD(s)/ds$. Again evaluating (12) by the residue theorem, we find for the detection probability

$$Q_d(\gamma) = D(1) \sum_{k=1}^{\infty} \frac{\rho_k^{(1)}(1 + 2\gamma\lambda_k + \gamma\lambda_k^2)}{(1+\gamma\lambda_k)(1+\lambda_k)D(\alpha_k)} \exp\left[-\frac{U_0}{\mu_k(\gamma)}\right], \tag{20}$$

where the coefficients

$$\rho_k^{(1)} = \lambda_k / D'(-\lambda_k^{-1}) = \prod_{\ell \neq k} \left(1 - \frac{\lambda_\ell}{\lambda_k}\right)^{-1}, \tag{21}$$

independent of γ, can be computed once for all values of the design s.n.r.

(b) The Threshold Detector

The threshold detection statistic U_θ is obtained by neglecting λ_k in the denominator of each term in (8), as though the signal for which the detector is designed to be optimum were much weaker than the noise,

$$U_\theta = (2N)^{-1} \sum_{k=1}^{\infty} \lambda_k |z_k|^2. \tag{22}$$

It is compared with a decision level U_0^θ, and a signal is declared present when $U_\theta > U_0^\theta$. The m.g.f. of the threshold statistic is

$$h_\gamma^\theta(s) = E[\exp(-sU_\theta)|H_\gamma]$$

$$= \prod_{k=1}^{\infty} [1 + \mu_k^\theta(\gamma)s]^{-1}$$

$$= [D(\alpha_s')D(\beta_s')]^{-1}, \tag{23}$$

$$\mu_k^\theta(\gamma) = \lambda_k(1+\gamma\lambda_k), \tag{24}$$

$$\alpha_s' = \frac{1}{2}[s + (s^2 - 4\gamma s)^{\frac{1}{2}}], \quad \beta_s' = \frac{1}{2}[s - (s^2 - 4\gamma s)^{\frac{1}{2}}], \tag{25}$$

A similar analysis shows that the detection probability attained by the threshold detector,

$$Q_d^\theta(\gamma) = \Pr(U_\theta > U_0^\theta | H_\gamma), \tag{26}$$

is given by the residue series (13) with μ_k replaced by μ_k^θ, or by

$$Q_d^{\theta} = \sum_{k=1}^{\infty} \frac{\rho_k^{(1)}(1+2\gamma\lambda_k)}{(1+\gamma\lambda_k)D(\alpha_k')} \exp\left[-\frac{U_0}{\mu_k^{\theta}(\gamma)}\right],$$

$$\alpha_k' = \gamma/(1+\gamma\lambda_k). \tag{27}$$

Here the parameter γ measures the signal strength relative to that of the signal S(t) involved in (1), although this is no longer that for which the detector is optimum.

(c) The Fredholm Determinant

The series in (20) and (27) are most convenient when the Fredholm determinant D(s) is known in closed form. As shown by Siegert [10], it can be calculated from the solution $h(t,s;u;\tau)$ of the integral equation

$$h(t,s;u;\tau) + uN^{-1}\int_0^{\tau} \phi(t,r)h(r,s;u;\tau)dr = uN^{-1}\phi(t,s),$$

$$0 < (r,s) < \tau, \qquad 0 < \tau < T, \tag{28}$$

whereupon

$$D(s) = \exp\left[\int_0^T h(t,t;s;t)dt\right]. \tag{29}$$

When the real and imaginary parts of the complex envelope S(t) of the signal can be modeled as the outputs of identical linear systems driven by independent white-noise generators of equal strength, the signal will be said to be <u>leucogenic</u>. The Fredholm determinant D(s) can then be calculated by a method given by Baggeroer [11]. This is the case, in particular, when the signal is a segment of a stationary random process with a narrowband spectral density $\Phi(\omega)$ that is a rational function of ω^2; the complex autocovariance function of the signal is

$$\phi(t,s) = \int_{-\infty}^{\infty} \Phi(\omega)e^{j\omega(t-s)}d\omega/2\pi.$$

(The origin of the ω-scale is the carrier frequency Ω.) The linear systems, described by state vectors of finite dimension, are then stationary, as are the white-noise generators. By utilizing a linear system with complex state variables, as shown by Van Trees [5, Appendix, pp. 565-598], a broader class of complex signal envelopes S(t) could be handled, but this has not been necessary in the work reported here. Once one has the Fredholm determinant, the eigenvalues λ_k can be calculated by finding its zeros s_k,

$$D(s_k) = 0, \quad \lambda_k = -1/s_k, \quad k = 1, 2, \ldots$$

When the real and imaginary parts of the signal envelope S(t) are independent Gauss-Markov processes, the complex autocovariance function is

$$\phi(t,s) = \phi_0 e^{-\mu|t-s|}, \tag{30}$$

the signal has a Lorentz spectral density

$$\Phi(\omega) = \frac{2\mu\phi_0}{\omega^2 + \mu^2}, \tag{31}$$

and as shown by Siegert [10] the Fredholm determinant is

$$D(s) = \frac{(1+g)^2 e^{mg} - (1-g)^2 e^{-mg}}{4ge^m},$$

$$g = (1+\kappa s)^{\frac{1}{2}}, \quad m = \mu T, \quad \kappa = \frac{2E}{mN}, \tag{32}$$

where $E = \phi_0 T$ is the average energy of the signals s(t). The eigenvalues λ_k are given by

$$\lambda_k = \kappa \sin^2 \theta_k, \tag{33}$$

where θ_k is a root of the transcendental equation

$$m \cot \theta_k = 2\theta_k + (k-1)\pi,$$

$$k = 1, 2, \ldots, \quad 0 < \theta_k < \pi/2, \tag{34}$$

which can quickly be solved by Newton's method. The associated value of g in

(32) is

$$g_k = j \cot \theta_k.$$

For $k >> 1$ the eigenvalues are approximately

$$\lambda_k \cong \frac{\kappa\pi^2}{m^2 + (k-1)^2\pi^2} = N^{-1} \Phi\left(\frac{(k-1)\pi}{T}\right). \tag{35}$$

In terms of θ_k the constants $\rho_k^{(1)}$ defined by (21) are

$$\rho_k^{(1)} = \frac{(-1)^{k-1} e^m \sin^2 2\theta_k}{m + 2\sin^2 \theta_k}. \tag{36}$$

For a stationary leucogenic signal whose narrowband spectral density $\Phi(\omega)$ has the form of that for the noise in an RLC circuit in thermal equilibrium, the Fredholm determinant has been calculated by Slepian [12].

(d) Computation with the Residue Series

When the eigenvalues λ_k drop off rapidly to zero with increasing index k, it is unnecessary to have the Fredholm determinant D(s) in closed form in order accurately to evaluate the residue series (13), (20), and (27), provided one has computed a sufficient number of those eigenvalues. The behavior of the eigenvalues illustrated by (35),

$$\lambda_k \cong N^{-1}\Phi(k\pi/T), \quad k >> 1,$$

is at least approximately manifested for arbitrary smooth spectral densities $\Phi(\omega)$, and the more rapidly the spectral density decreases to zero with increasing angular frequency ω, the more expeditious computation with the residue series becomes.

When the narrowband spectral density $\Phi(\omega)$ is a rational function of ω^2, the eigenvalues λ_k can be calculated by methods given by Youla [13], the writer [14], Slepian and Kadota [15], and Baggeroer [11]. The method of [11] applies

also to nonstationary leucogenic signals.

In the extreme case of bandlimited signals with a rectangular spectral density

$$\Phi(\omega) = E/W, \qquad -\pi W < \omega < \pi W,$$
$$= 0, \qquad |\omega| > \pi W, \tag{37}$$

of bandwidth W, the eigenfunctions $f_k(t)$ are the prolate spheroidal wavefunctions [16], and the eigenvalues have been tabulated by Slepian and Sonnenblick [17]. Their eigenvalues, which we denote by λ_n^s, are related to those as defined here by

$$\lambda_n = \frac{E}{NWT}\,\lambda_{n-1}^s, \tag{38}$$

and their parameter c is

$$c = \pi WT/2. \tag{39}$$

Reference [17] tabulates λ_n^s for $0 \le n \le 20$ and n = 25, 30, 35, 40, and for integral values of c up to 20, as well as for c = 25, 30, 35, 40. For $c >> 1$ there are approximately WT equal eigenvalues $\lambda_k \cong E/(NWT)$, and the rest decrease exponentially to zero with increasing index k.

For the sake of comparing spectral densities we adopt as our definition of bandwidth W the expression

$$W = \left[\int_{-\infty}^{\infty} \Phi(\omega)\,d\omega/2\pi\right]^2 \Big/ \int_{-\infty}^{\infty} [\Phi(\omega)]^2 d\omega/2\pi, \tag{40}$$

which accords with (37). For the Lorentz spectral density in (31), W = μ. The effective number

$$M = \left(\sum_{k=1}^{\infty} \lambda_k\right)^2 \Big/ \sum_{k=1}^{\infty} \lambda_k{}^2 \tag{41}$$

of significant eigenvalues of (5) is

$$M = [\overline{\phi}(0)T]^2 \Big/ \int_{-\frac{1}{2}T}^{\frac{1}{2}T} \int_{-\frac{1}{2}T}^{\frac{1}{2}T} |\overline{\phi}(t-u)|^2 dt\,du \tag{42}$$

in terms of the complex autocovariance function $\overline{\phi}(\tau) = \phi(t,t+\tau)$ for a stationary signal, and it is approximately equal to the time-bandwidth product WT when large.

When the time-bandwidth product is large, computation with the residue series (13), (20), and (27) becomes infeasible. Its terms alternate in sign, and as the terms of lowest order are of the same order of magnitude, they must be evaluated with high precision if the series is to be accurately summed. The constants ρ_k in (13) and $\rho_k^{(1)}$ in (20) and (27) involve differences of the eigenvalues, and because the eigenvalues of lowest order lie close together, these must be known to many significant figures in order to determine those constants accurately. The situation is least favorable for the rectangular spectral density, for which the eigenvalues are tabulated to only eight significant figures, and computing them to more significant figures would be laborious. Even for the Lorentz spectral density, the residue series has been found to be inaccurate for WT of the order of 10 or larger. Another method of evaluating the detection probability $Q_d(\gamma)$ must be sought.

III. Steepest Descent Integration

When summing the residue series is not feasible, we resort instead to evaluating the integral in (12) or its counterpart

$$1 - Q_d(\gamma) = Q_1(\gamma) = \int_{c-i\infty}^{c+i\infty} s^{-1} h_\gamma(s) \exp(U_0 s)\, ds/2\pi j, \qquad c > 0, \tag{43}$$

numerically. We have a broad latitude in picking the location and the form of the contour of integration, and we try to choose them in the most advantageous manner. Viewed as a function of s for real values of s in $-\mu_1^{-1} < \mathrm{Re}\ s < \infty$, the integrand

$$\exp \Psi(s) = (\pm s)^{-1} h_\gamma(s) \exp(U_0 s) \tag{44}$$

of (12) or (43) has two minima, one at a point $s = u_0'$ in $-\mu_1^{-1} < \mathrm{Re}\ s < 0$, the other at a point $s = u_0'' > 0$. (For $\pm s$ we use $-s$ when the path of integration passes through u_0' and (12) is evaluated, and we use $+s$ when the path passes through u_0'' and (43) is evaluated.) As a function of complex values of s, the integrand has saddlepoints at u_0' and u_0'' [6]. If the path of integration passes vertically through u_0' or u_0'', the magnitude of the integrand, which is maximum at the saddlepoint, decreases most rapidly as the point $s = u + jv$ moves up or down the contour from u_0' or u_0''.

These saddlepoints are the roots of the equation

$$\Psi'(u_0) = \frac{d}{ds}\left[\ln h_\gamma(s)\right]\Big|_{s=u_0} + U_0 - u_0^{-1} = 0,$$

$$u_0 = u_0',\ u_0'', \tag{45}$$

primes on Ψ denoting differentiation, and this equation can be expeditiously solved by Newton's method,

$$u_0 \leftarrow u_0 - \frac{\Psi'(u_0)}{\Psi''(u_0)},$$

$$\Psi''(u_0) = \frac{d^2}{ds^2}\,[\ln h_\gamma(s)]\Big|_{s=u_0} + u_0^{-2} > 0 \tag{46}$$

It will be necessary to compute these derivatives numerically if the Fredholm determinant D(s) involved in $h_\gamma(s)$ is not known in closed form or is too complicated. Alternatively one can use Newton's method to solve the equation

$$\text{Im}\ \Psi(u+jv) = 0 \tag{47}$$

for u, with the imaginary part v taken infinitesimal, but positive, evaluating the derivative of this function numerically. The values of u_0' and u_0'' need not be known to high precision.

In [6] the integrals in (12) and (43) were evaluated approximately as

$$Q_d(\gamma) \cong [2\pi\Psi''(u_0')]^{-\frac{1}{2}} \exp \Psi(u_0') \tag{48}$$

when $U_0 > E(U|H_\gamma)$, $u_0' < 0$, and

$$1 - Q_d(\gamma) \cong [2\pi\Psi''(u_0'')]^{-\frac{1}{2}} \exp \Psi(u_0''), \tag{49}$$

when $U_0 < E(U|H_\gamma)$, $u_0'' > 0$. That paper [6] lists previous work on "saddlepoint approximations" of this kind.

The path along which the integrand in (12) and (43) decreases most rapidly to zero is called the path of steepest descent [8]. Along the path of steepest descent the integrand remains real, or what is the same thing,

$$\text{Im}\ \Psi(s) = \arg h_\gamma(s) + U_0 s - \arg(\pm s) = 0, \qquad s = u + jv, \tag{50}$$

where arg s is the principal value of Im (ℓn s). Because the integrand decreases most rapidly along this path, a numerical integration of (12) or (43) along it, utilizing, let us say, the trapezoidal rule, requires fewest steps in order to attain a prescribed accuracy. Solving (50) precisely at each point along the path at which the integrand is evaluated, however, would much protract

the computation. Instead we solve (50) only approximately and correct for the discrepancy.

Equal steps Δv are taken in the vertical direction, starting at $v = 0$. For each value $v = v_m = m\Delta v$, $m = 1, 2, \ldots$, the solution of (50) for $u = u(v_m)$ is undertaken by Newton's method. That is, with a convenient interval δu, and starting with a trial value of u, we determine a new trial value by

$$u \leftarrow u - \frac{f(u)\delta u}{f(u+\delta u) - f(u)}, \qquad f(u) = \operatorname{Im} \Psi(u + jv). \tag{51}$$

In our computations the number of iterations at each point was limited to five. The initial trial value was taken as the linear extrapolation of the two previous solutions,

$$u \leftarrow 2u(v_{m-1}) - u(v_{m-2}).$$

(A quadratic extrapolation,

$$u \leftarrow 3u(v_{m-1}) - 3u(v_{m-2}) + u(v_{m-3}),$$

would start the iterations of Newton's method closer to the solution of (50) and reduce the number of iterations required.)

The trapezoidal rule is used for reasons explained by Rice [7]. By virtue of the symmetry of the integrand and the path of integration with respect to the real axis, we approximate the integral by

$$\left.\begin{aligned} u_0 &= u_0' < 0, \quad Q_d(\gamma) \\ u_0 &= u_0'' > 0, \quad 1 - Q_d(\gamma) \end{aligned}\right\} = \frac{1}{\pi} \operatorname{Re} \sum_{m=0} \varepsilon_m \exp\left[\Psi(s_m)\right](\Delta v - j\Delta u),$$

$$s_m = u(v_m) + jv_m, \qquad v_m = m\Delta v,$$

$$\Delta u = u(v_m) - u(v_{m-1}), \qquad m > 0$$

$$= 0, \qquad m = 0,$$

$$\varepsilon_m = \begin{cases} \frac{1}{2}, & m = 0 \\ 1, & m > 0. \end{cases} \tag{52}$$

As with the saddlepoint approximation in (48), (49), the integration starts from $u_0' < 0$ for $U_0 > E(U|H_\gamma)$ and from $u_0'' > 0$ for $U_0 < E(U|H_\gamma)$. When the decision level U_0 is close to the mean $E(U|H_\gamma)$, it does not matter at which saddlepoint the integration begins. The summation is stopped when the magnitude $\exp[\mathrm{Re}\ \Psi(s_m)]$ of the integrand falls below a specified fraction of the value of the sum so far accumulated.

If (50) were solved exactly, the factor $\exp \Psi(s_m)$ in (52) would be real and the term $j\Delta u$ in $\Delta s = \Delta v - j\Delta u$ would not contribute, but since (50) is solved only approximately in order to save computer time, $\Psi(s_m)$ has a small imaginary part, which combined with $j\Delta u$ induces a small, but necessary correction to the terms of (52).

The initial step-size was taken as

$$\Delta v = \left|2\Psi''(u_0)\right|^{-\frac{1}{2}}, \qquad u_0 = u_0' \text{ or } u_0'', \tag{53}$$

which is of the order of magnitude of the width of the integrand as a function of v in the vertical direction. The second derivative $\Psi''(u_0)$ arises in solving (45) to determine the saddlepoint and is thus known before integration begins.

Figures 1 and 2 show typical paths of steepest descent for calculating the probabilities $Q_0 = Q_d(0)$ and $Q_1(1) = 1 - Q_d(1)$ for the optimum detectors of stochastic signals having Lorentz and rectangular spectra, respectively. The negative numbers along the paths indicate $\log_{10}$ of the ratio of the value of the integrand at each marked point to that at the saddlepoint. The rapid decrease in the integrand is evident.

By expanding the exponent $\Psi(s)$ of the integrand in (12) or (43) in a power series about the saddlepoint and keeping terms through $(s - u_0)^4$, one finds for the equation of the path of steepest descent in that region

$$v^2 = \frac{\upsilon(6\Psi_0'' + 3\Psi_0'''\,\upsilon + \Psi_0''''\,\upsilon^2)}{\Psi_0''' + \Psi_0''''\upsilon}, \qquad \upsilon = u - u_0, \tag{54}$$

the primes indicating derivatives of $\Psi(s)$, which are evaluated at u_0. Thus in the neighborhood of the saddlepoint the path is approximately a parabola [18],

$$u = u_0 - \tfrac{1}{2}\sigma v^2, \qquad \sigma = -\Psi_0'''/3\Psi_0''. \tag{55}$$

Having determined that the path of steepest descent is nearly parabolical, one can shorten the computation time by integrating instead along the curve defined by (55), replacing (52) by

$$\left.\begin{aligned} u_0 &= u_0' < 0, \qquad Q_d(\gamma) \\ u_0 &= u_0'' > 0, \quad 1 - Q_d(\gamma) \end{aligned}\right\} = \frac{1}{\pi}\,\mathrm{Re}\sum_{m=0}^{\infty} \varepsilon_m \exp[\Psi(s_m)](1 + j\sigma v_m)\Delta v,$$

$$v_m = m\Delta v, \qquad s_m = u_0 - \tfrac{1}{2}\sigma v_m^2 + jv_m, \qquad \varepsilon_m = \begin{cases} \frac{1}{2}, & m = 0 \\ 1, & m > 0. \end{cases} \tag{56}$$

It is unnecessary to know the curvature σ to high accuracy, and if it is inconvenient to differentiate $\Psi(s)$ analytically at $s = u_0$, one can determine σ numerically by evaluating the exponent $\Psi(s)$ at two points on each side of the saddlepoint:

$$\psi_k = \Psi(u_0 + k\delta), \qquad k = -2, -1, 1, 2,$$

whereupon fitting a third-degree polynomial to these points yields the approximation

$$\sigma \doteq \frac{2(\psi_1 - \psi_{-1}) - \psi_2 + \psi_{-2}}{2\delta(\psi_2 + \psi_{-2} - \psi_1 - \psi_{-1})} \tag{57}$$

One can take the spacing δ of the order of Δv as given by (53).

Trials with both (52) and (56) with the same design s.n.r. $S_0 = E/N$ for values of the time-bandwidth product WT equal to 4, 8, 12, 20, and 35, with the decision level U_0 selected to yield a false-alarm probability of 10^{-4} and with the spacing Δv selected as in (53), yielded identical results to eight significant figures. With the integration stopped when the magnitude $\exp[\mathrm{Re}\,\Psi(s)]$ fell to 10^{-10} times the value of the accumulated sum, eleven steps were required.

Halving the step-size changed the result only in the eighth significant figure, and only once by more than one digit in that place; twenty or twenty-one steps were required. The curvature σ decreased slightly as WT increased from 4 to 35.

Integration for $Q_d(0)$ and $Q_d(1)$ along the path in Fig. 2 for the rectangular spectral density and along the approximating parabola (55) yielded results stable to seven significant figures with eight steps.

IV. Setting the Decision Level

The decision level U_0 is to be set at such a value that a pre-assigned false-alarm probability

$$Q_0 = Q_d(0) = \int_{U_0}^{\infty} p_0(U)dU \tag{58}$$

is attained; $p_0(U)$ is the probability density function of the statistic U under hypothesis H_0 that no signal is present. Starting from a trial value of U_0, a new trial value can be computed by Newton's method,

$$U_0 \leftarrow U_0 - \frac{Q_d(0) - Q_0}{p_0(U_0)}, \tag{59}$$

and the procedure repeated until the value of U_0 ceases changing significantly.

The residue series for the terms in (55) is from (20)

$$Q_d(0) = D(1) \sum_{k=1}^{\infty} \frac{\rho_k^{(1)}}{1+\lambda_k} \exp\left[-\frac{(1+\lambda_k)U_0}{\lambda_k}\right] \tag{60}$$

and by differentiation

$$p_0(U_0) = D(1) \sum_{k=1}^{\infty} \frac{\rho_k^{(1)}}{\lambda_k} \exp\left[-\frac{(1+\lambda_k)U_0}{\lambda_k}\right] \tag{61}$$

When the time-bandwidth product WT is so large that computation with the residue series is infeasible, the probability $Q_d(0)$ can be calculated by integrating (12) with $\gamma = 0$ along the path of steepest descent or along a parabola as in (56). The density function $p_0(U)$ is given by a similar contour integral

$$p_0(U) = \int_C h_0(s)e^{Us}ds/2\pi j. \tag{62}$$

Although it is not the best contour for evaluating (62), the steepest-descent path used for evaluating (12), as explained in Section III, or the parabola

in (55), can be used to integrate (62) numerically as well; the computer accumulates both sums simultaneously. The value of $p_0(U_0)$ in (59) is not needed to great accuracy in order for Newton's method to be applied.

Computer time can be saved by determining the initial trial value of U_0 by the more rapidly calculated saddlepoint approximation in (48), which for this purpose takes the form

$$Q_0 \cong \left|2\pi\Psi_0''(u_0')\right|^{-\frac{1}{2}} \frac{D(1)}{|u_0'|D(u_0'+1)} \exp\,(U_0u_0') \tag{63}$$

with

$$\exp\,[\Psi_0(s)] = \frac{D(1)}{sD(s+1)} \exp\,(U_0s). \tag{64}$$

Solved for U_0, (63) yields

$$U_0 = u_0'^{-1}\ell n\{\left|2\pi\Psi_0''(u_0')\right|^{\frac{1}{2}}|u_0'|D(u_0'+1)Q_0/D(1)\}. \tag{65}$$

One puts a crude trial value of the decision level U_0 into (45), determines the saddlepoint $u_0' < 0$, calculates a new trial value of U_0 from (65), and iterates this procedure until it converges; it has been found to do so rapidly. The result is the initial trial value of U_0 for (59).

V. Performance of the Optimum and Threshold Detectors

Equipped now with accurate means of calculating the detection probability $Q_d(\gamma)$ for a range of values of the time-bandwidth product WT, we can compare the performance of detectors designed to be optimum for various values of the design s.n.r. $S_0 = E/N$, including the threshold detector, for which that design s.n.r. equals zero. We set the false-alarm probability $Q_0 = Q_d(0)$ equal to 10^{-4} and determined the decision levels U_0 as described in Section IV. The input s.n.r. $S = \gamma S_0$ required to attain detection probabilities $Q_d(\gamma) = \overline{Q}_d = 0.9$, 0.99, 0.999, and 0.9999 were then computed by Newton's method. That is, with a suitable increment $\delta\gamma$, a new trial value of the ratio γ was determined by

$$\gamma \leftarrow \gamma - \frac{Q_d(\gamma) - \overline{Q}_d}{Q_d(\gamma + \delta\gamma) - Q_d(\gamma)} \delta\gamma$$

in which the values of $Q_d(\gamma)$ and $Q_d(\gamma + \delta\gamma)$ were determined by either the residue series, as in Section II, or the contour integral, as in Section III, depending on whether the time-bandwidth product WT was small or large.

The resulting input s.n.r. $S = \gamma S_0$ are plotted in db. in Figs. 3 - 7 versus the s.n.r. S_0 for which the receiver is designed to be optimum. Figures 3 and 4 display the results for signals with Lorentz and rectangular spectral densities, respectively, and with the same time-bandwidth product $WT = 8/\pi = 2.5465$. Figures 5 and 6 do the same for $WT = 14/\pi = 4.4563$. (These values of WT correspond to values of Slepian's parameter c equal to 4 and 7, respectively.) Figure 7 displays the input s.n.r. for signals with a Lorentz spectral density and WT = 35.

Each of the curves in these figures exhibits a minimum at that value of the design s.n.r. S_0 for which $Q_d(1)$ equals the fixed detection probability $\overline{Q}_d$ for the curve. For larger design s.n.r. the curves rise extremely slowly; in this range the performance is quite insensitive to the s.n.r. for which the detector is designed to be optimum. For smaller design s.n.r., on the other hand, the

curves rise rapidly to their peak value at $S_0 = 0$, which represents the threshold detector. The difference between that peak value and the minimum measures the relative performance disadvantage of the threshold detector.

This relative disadvantage is much smaller for signals with a rectangular spectral density than for signals with a Lorentz spectral density, for equal values of the time-bandwidth product WT. The reason is easily seen. Because for the rectangular spectral density the integral equation (5) has approximately WT equal eigenvalues λ_k, and the rest are negligible, the optimum detector is very like a detector that employs the decision statistic

$$U' = \sum_{k=1}^{[WT]} |z_k|^2$$

for all values of the design s.n.r., where [WT] is the integral part of WT. That this is a good approximation is evident from (8). The statistic U' has approximately a scaled chi-squared distribution with 2[WT] degrees of freedom. The performance of the optimum detector for signals with a rectangular spectral density, therefore, does not vary much over the entire range of values of the design s.n.r. For signals with a Lorentz spectral density, on the other hand, the relative weighting of the terms in (8) is far from uniform and depends more strongly on the design s.n.r. As Fig. 7 shows, even at WT = 35 the difference between the threshold detector and the detector optimum at each of the prescribed values $\bar{Q}_d$ of $Q_d(1)$ is of the order of 0.65 db. Although the threshold detector is close to the optimum when the s.n.r. per degree of freedom, E/(NWT), is small, the weak-signal approximation by which it is derived becomes valid for signals with a sharply cut-off spectral density at lower values of the time-bandwidth product WT than for signals whose spectral density declines only slowly to zero with increasing frequency deviation $|\omega|$.

It was the efficiency of numerically integrating the Laplace inversion integrals in (12) and (43) along the path of steepest descent or its osculatory parabola that enabled computing in a reasonable time the great number of values of the detection probability $Q_d(\gamma)$ needed for mapping the performance of these detectors to the extent described here. The method is worthy of trial whenever cumulative probabilities are to be evaluated for random variables whose moment-generating or characteristic functions are known in analytic or computable form.

ACKNOWLEDGMENT

I am indebted to Dr. Stephen O. Rice for instructive and stimulating discussions of these problems and techniques.

REFERENCES

[1] J. V. di Franco and W. L. Rubin, Radar Detection, Englewood Cliffs, N.J.: Prentice-Hall, 1968. See Chapter 11.

[2] R. Price and P. E. Green, Jr., Signal Processing in Radar Astronomy -- Communication via Fluctuating Multipath Media, M.I.T. Lincoln Lab., Tech. Report no. 234, October 6, 1960.

[3] D. Middleton, Statistical Communication Theory, New York: McGraw-Hill, 1960. See Sec. 20.4.

[4] C. W. Helstrom, Statistical Theory of Signal Detection, 2nd ed., New York: Pergamon, 1968. See Chapter XI.

[5] H. L. Van Trees, Detection, Estimation, and Modulation Theory, vol. 3, New York: Wiley, 1971. See Chapter 4.

[6] C. W. Helstrom, "Approximate evaluation of detection probabilities in radar and optical communications," IEEE Trans. on Aerospace & Electronic Systems, vol. AES-14, pp. 630-640, July, 1978.

[7] S. O. Rice, "Efficient evaluation of integrals of analytic functions by the trapezoidal rule," Bell System Tech. J., vol. 52, pp. 707-722, May-June, 1973.

[8] G. F. Carrier, M. Krook, C. E. Pearson, Functions of a Complex Variable, New York: McGraw-Hill, 1966. See Sec. 6-3, pp. 257-266.

[9] R. E. Esch, "The instability of a shear layer between two parallel streams," J. Fluid Mech., vol. 3, pp. 289-303, 1957.

[10] A. J. F. Siegert, "A systematic approach to a class of problems in the theory of noise and other random phenomena -- Part II, Examples," I.R.E. Trans. on Inform. Theory, vol. IT-3, pp. 38-44, March, 1957.

[11] A. B. Baggeroer, "A state-variable approach to the solution of Fredholm integral equations," IEEE Trans. on Inform. Theory, vol. IT-15, pp. 557-570, September, 1969.

[12] D. Slepian, "Fluctuations of random noise power," Bell System Tech. J., vol. 37, pp. 163-184, January, 1958.

[13] D. Youla, "The solution of the homogeneous Wiener-Hopf integral equation occurring in the expansion of second-order random functions," I.R.E. Trans. on Inform. Theory, vol. IT-3, pp. 187-193, September, 1957.

[14] C. W. Helstrom, "Solution of the detection integral equation for stationary filtered white noise," IEEE Trans. on Inform. Theory, vol. IT-11, pp. 335-339, July, 1965.

[15] D. Slepian and T. Kadota, "Four integral equations of detection theory," SIAM J. Appl. Math., vol. 17, pp. 1102-1117, November, 1969.

[16] D. Slepian and H. O. Pollak, "Prolate spheroidal wave functions, Fourier analysis and uncertainty - I," Bell System Tech. J., vol. 40, pp. 65-84, 1961.

[17] D. Slepian and E. Sonnenblick, "Eigenvalues associated with prolate spheroidal wavefunctions of zero order," Bell System Tech. J., vol. 44, pp. 1745-1760, October, 1965.

[18] S. O. Rice, private communication.

Figure Captions

Fig. 1. Paths of steepest descent in contour integration of (12) for $Q_d(0)$, $Q_d(1)$: Lorentz spectral density, WT = 8, $S_0 = 100$, $U_0 = 34.849121$, $Q_0 = 10^{-4}$.

Fig. 2. Paths of steepest descent in contour integration of (12) for $Q_d(0)$, $Q_d(1)$: rectangular spectral density, WT = $14/\pi = 4.4563$, $S_0 = 100$, $U_0 = 18.195885$, $Q_0 = 10^{-4}$.

Fig. 3. Input s.n.r. to yield detection probability Q_d for $Q_0 = 10^{-4}$, versus design s.n.r. S_0: Lorentz spectral density, WT = $8/\pi = 2.5465$. Curves are indexed with the value of $\overline{Q}_d$.

Fig. 4. Input s.n.r. to yield detection probability $\overline{Q}_d$ for $Q_0 = 10^{-4}$, versus design s.n.r. S_0: rectangular spectral density, WT = $8/\pi = 2.5465$. Curves are indexed with the value of $\overline{Q}_d$.

Fig. 5. Input s.n.r. to yield detection probability $\overline{Q}_d$ for $Q_0 = 10^{-4}$, versus design s.n.r. S_0: Lorentz spectral density, WT = $14/\pi = 4.4563$. Curves are indexed with the value of $\overline{Q}_d$.

Fig. 6. Input s.n.r. to yield detection probability $\overline{Q}_d$ for $Q_0 = 10^{-4}$, versus design s.n.r. S_0: rectangular spectral density, WT = $14/\pi = 4.4563$. Curves are indexed with the value of $\overline{Q}_d$.

Fig. 7. Input s.n.r. to yield detection probability $\overline{Q}_d$ for $Q_0 = 10^{-4}$, versus design s.n.r. S_0: Lorentz spectral density, WT = 35. Curves are indexed with the value of $\overline{Q}_d$.

FOOTNOTES

Manuscript received ; revised

Publication of this research was partially supported by the Air Force Office of Scientific Research under Grant AFOSR-82-0343. Author's address: Department of Electrical Engineering and Computer Sciences, University of California, San Diego; La Jolla, California 92093.

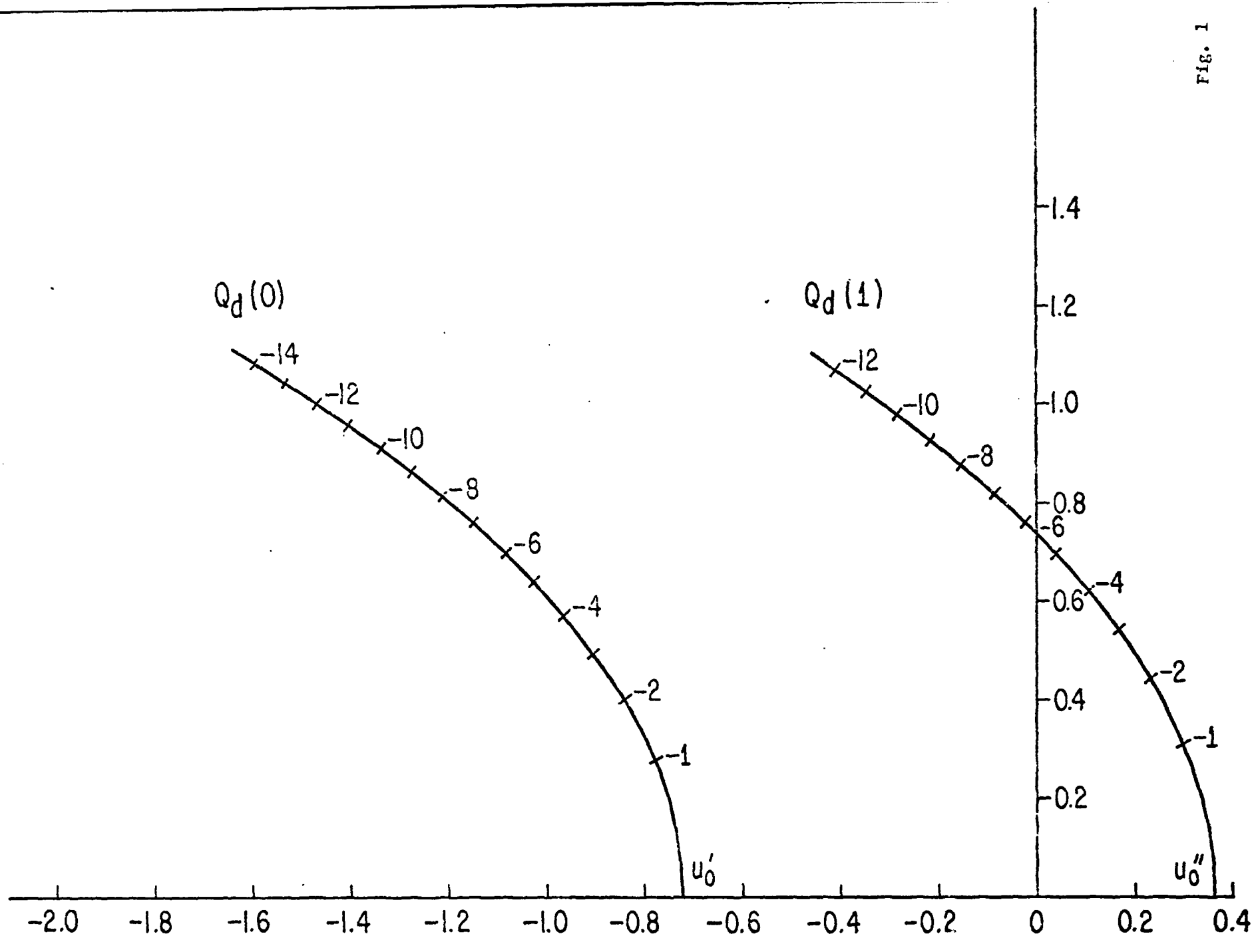
$Q_d(0)$
-14
-12
-10
-8
-6
-4
-2
-1
u_0'
$Q_d(1)$
-12
-10
-8
-6
-4
-2
-1
u_0''
1.4
1.2
1.0
0.8
0.6
0.4
0.2
-2.0
-1.8
-1.6
-1.4
-1.2
-1.0
-0.8
-0.6
-0.4
-0.2
0
0.2
0.4

Fig. 1

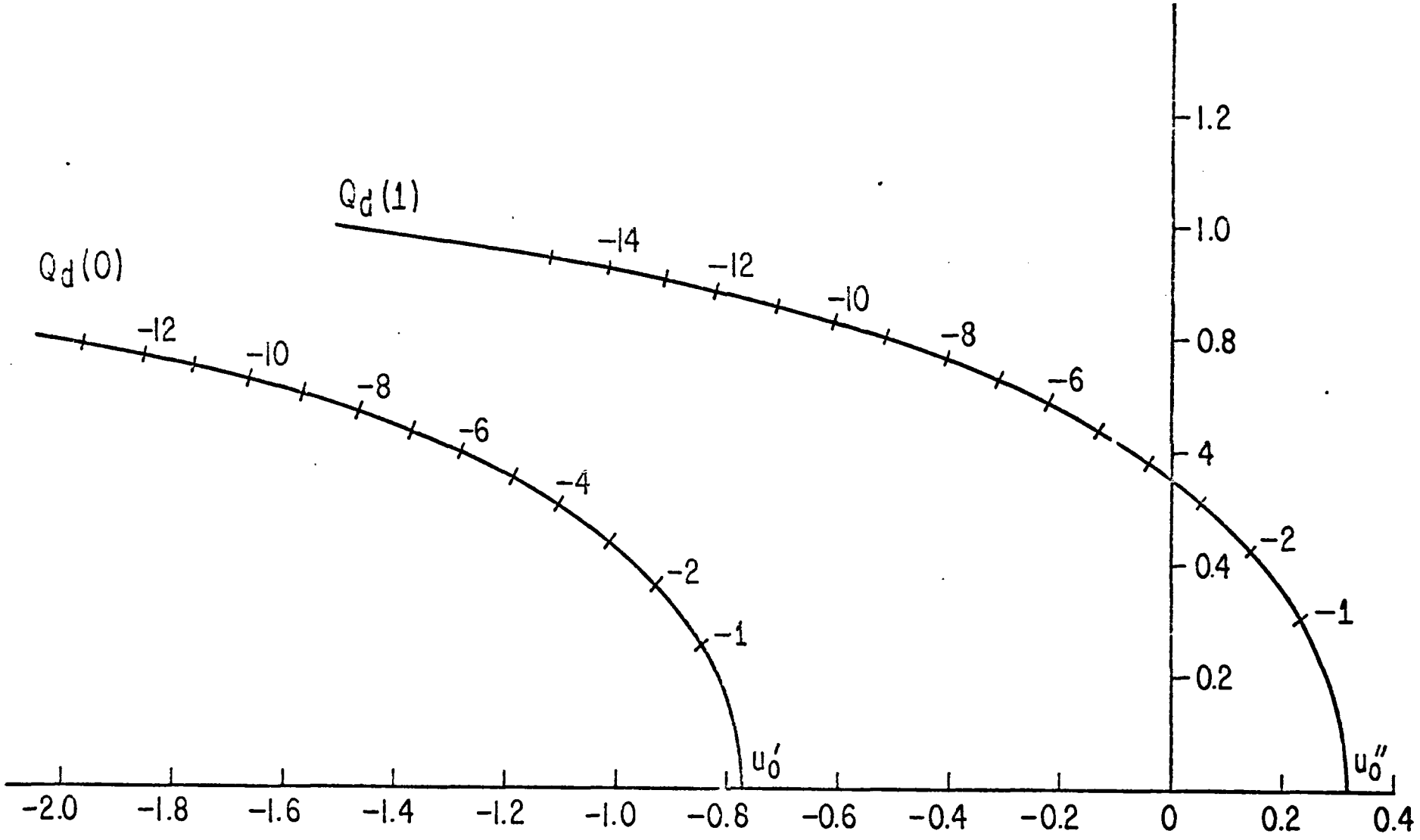
$Q_d(1)$
$Q_d(0)$
-14
-12
-10
-8
-6
-4
-2
-1
1.2
1.0
0.8
0.4
0.2
u_0'
u_0''
-2.0
-1.8
-1.6
-1.4
-1.2
-1.0
-0.8
-0.6
-0.4
-0.2
0
0.2
0.4

Fig. 2

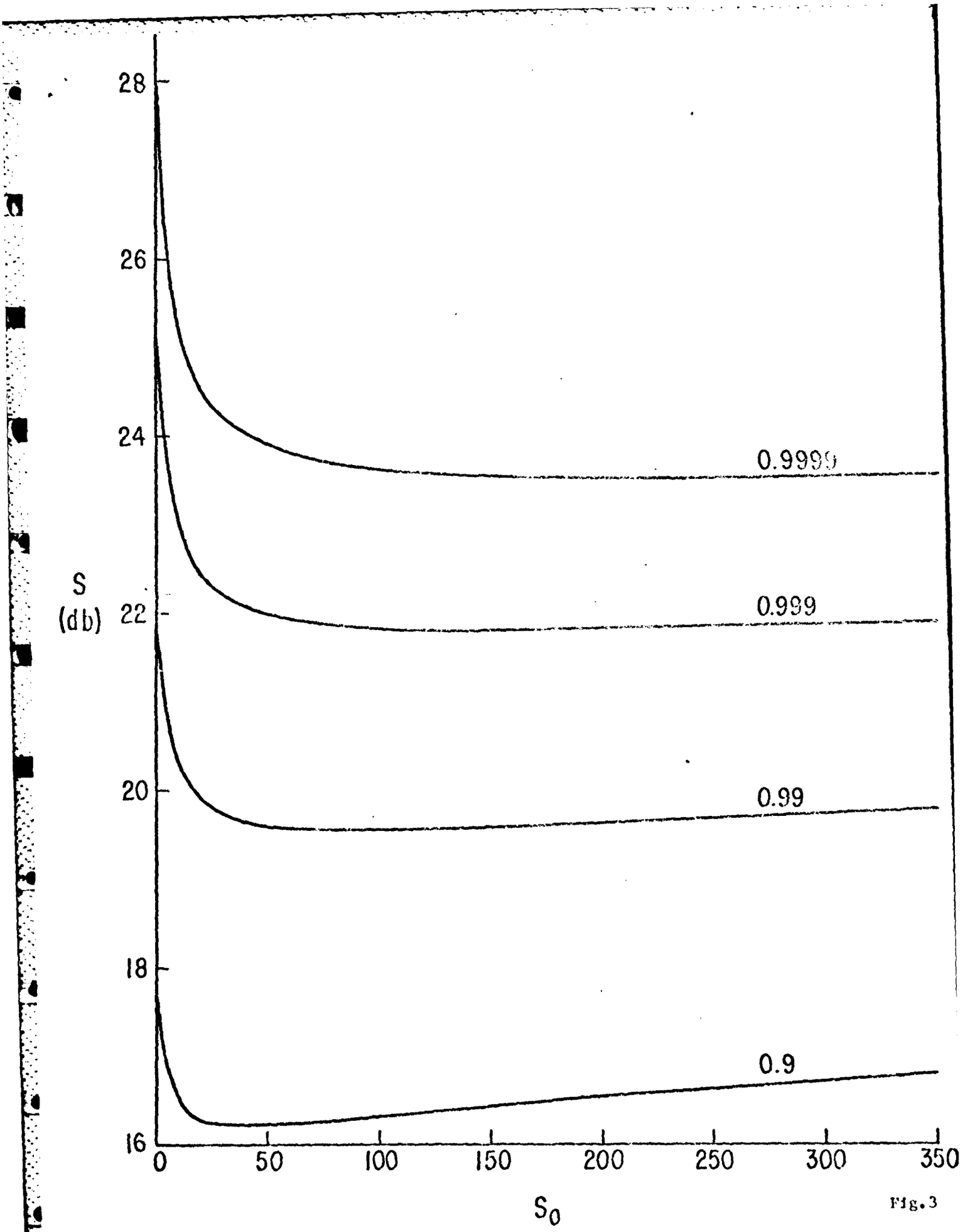
28
26
24
22
20
18
16
S
(db)
0.9999
0.999
0.99
0.9
0
50
100
150
200
250
300
350
S_0

Fig.3

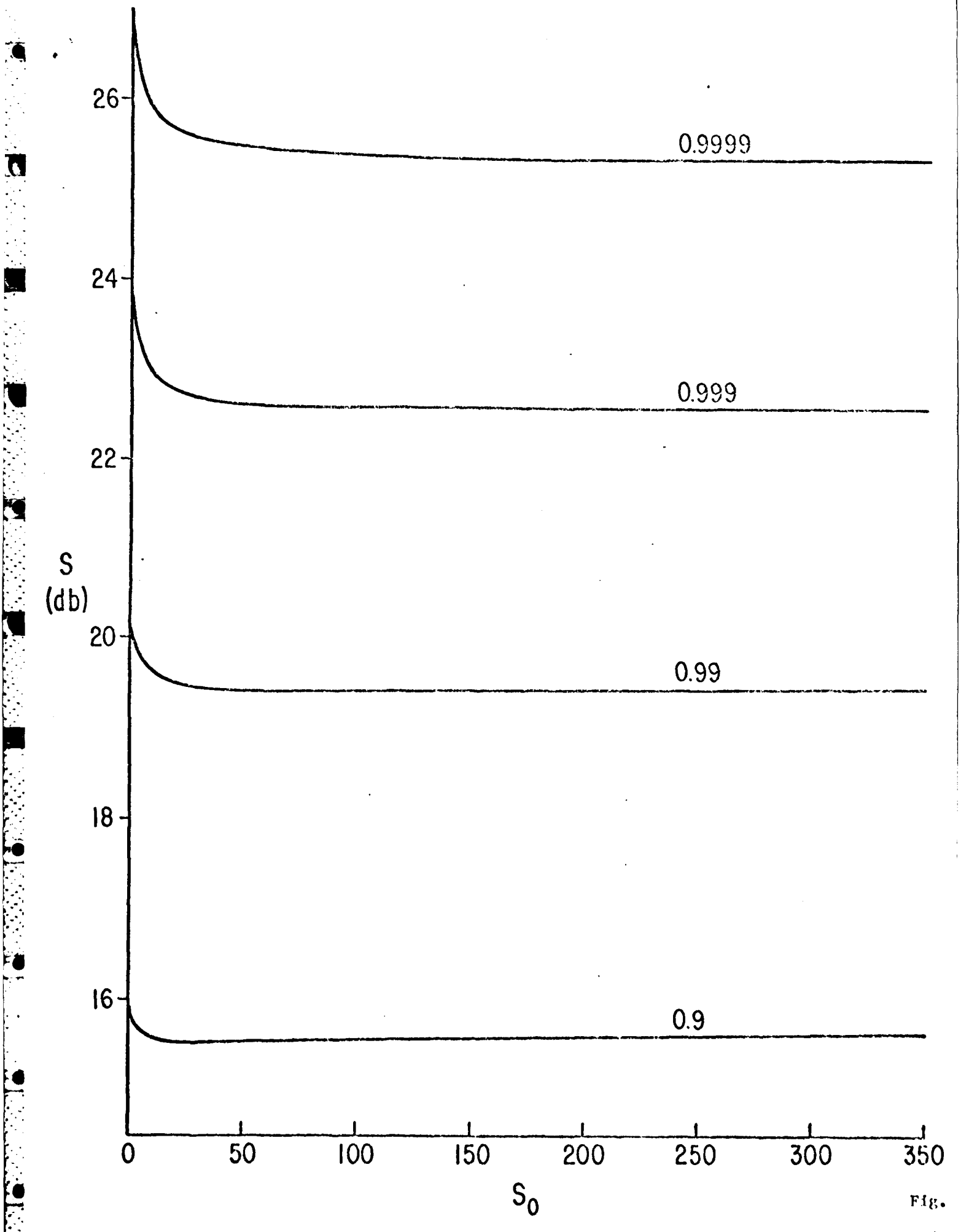
26
24
22
20
18
16
S
(db)
0.9999
0.999
0.99
0.9
0
50
100
150
200
250
300
350
S_0

Fig.

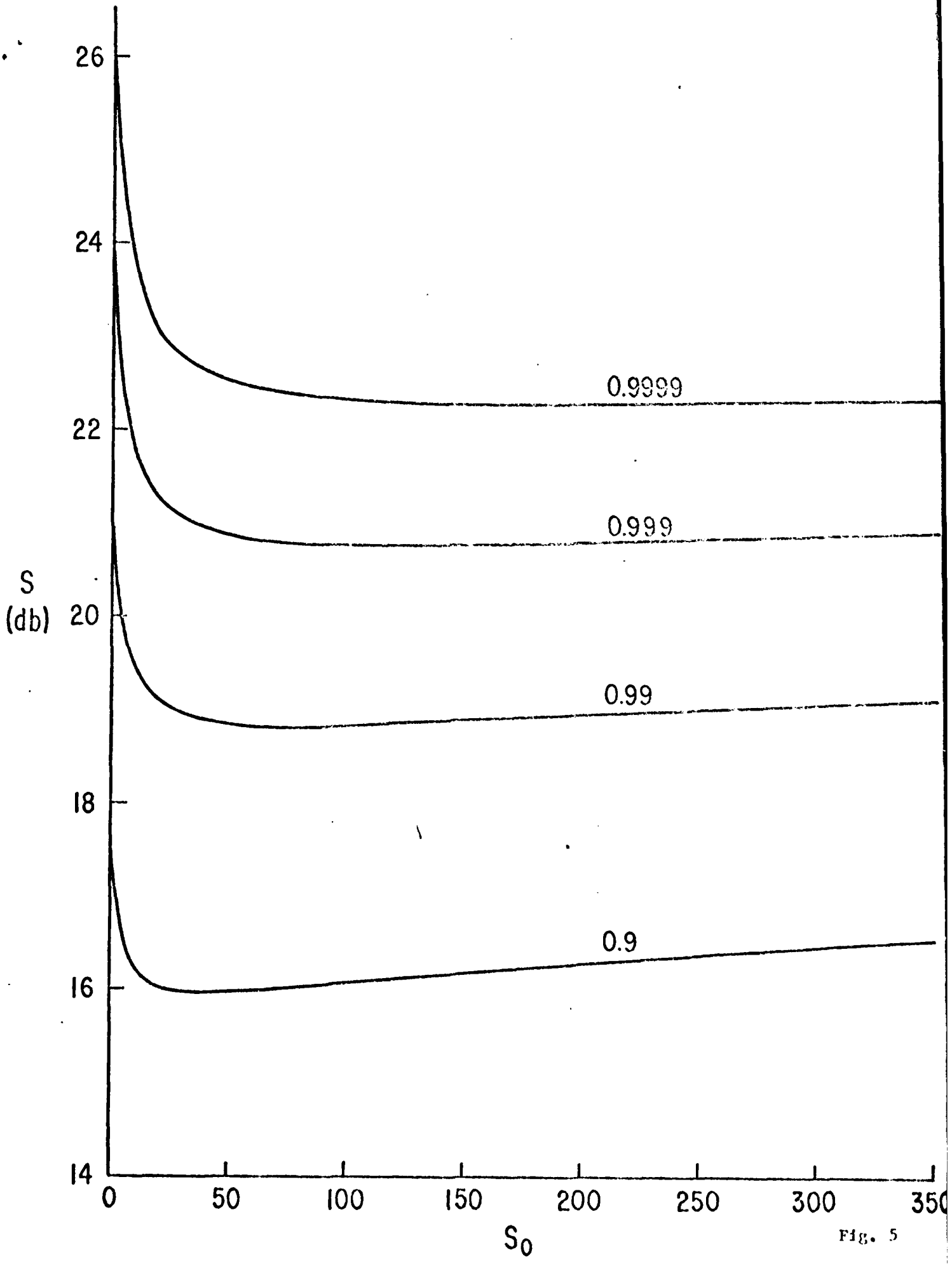
26
24
22
20
18
16
14
S
(db)
0.9999
0.999
0.99
0.9
0
50
100
150
200
250
300
350
S_0

Fig. 5

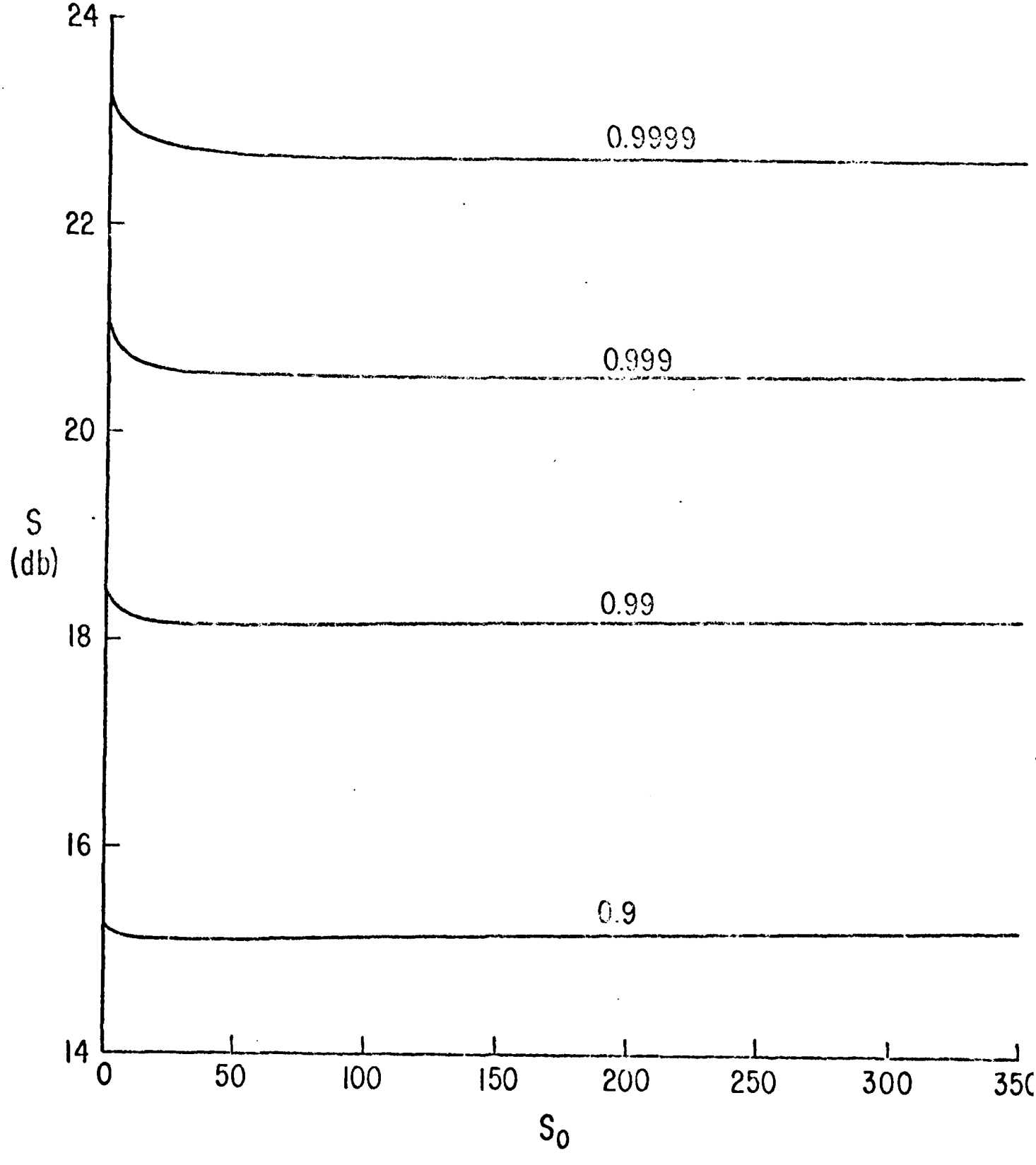
24
22
20
18
16
14
S
(db)
0.9999
0.999
0.99
0.9
0
50
100
150
200
250
300
350
S_0

Fig. 6

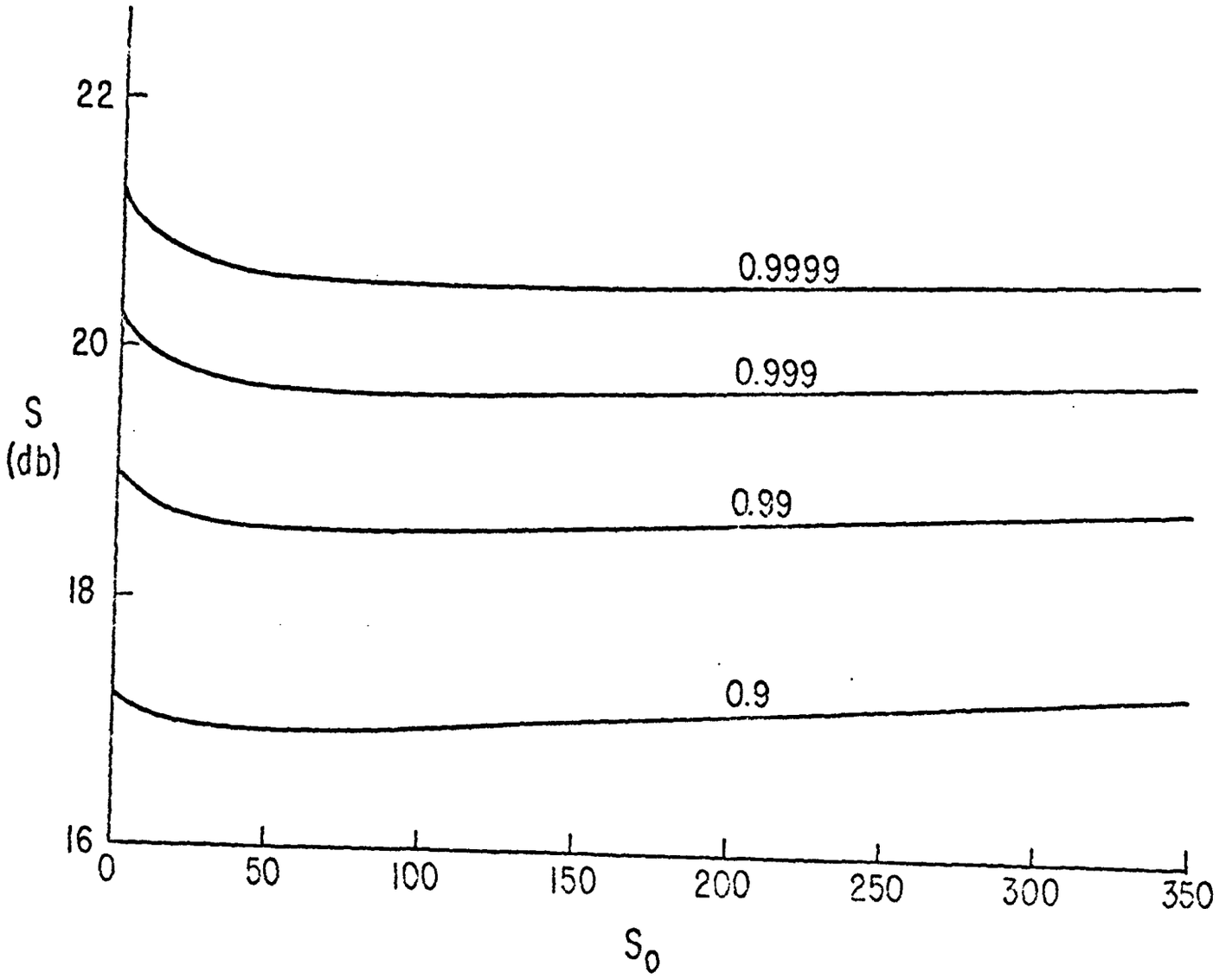

Fig. 7

END

FILMED

6-83

DTIC